Arachidonic acid mediates muscarinic inhibition and enhancement of N-type Ca^{2+} current in sympathetic neurons

Liwang Liu and Ann R. Rittenhouse*

Program in Neuroscience, Program in Cellular and Molecular Physiology, Department of Physiology, University of Massachusetts Medical School, 55 Lake Avenue North, Worcester, MA 01655

N-type Ca^{2+} channels participate in acute activity-dependent processes such as regulation of Ca^{2+}-activated K$^+$ channels and in more prolonged events such as gene transcription and long-term depression. A slow postsynaptic M$_1$ muscarinic receptor-mediated modulation of N-type current in superior cervical ganglion neurons may be important in regulating these processes. This slow pathway inhibits N-type current by using a diffusible second messenger that has remained unidentified for more than a decade. Using whole-cell patch–clamp techniques, which isolate the slow pathway, we found that the muscarinic agonist oxotremorine methiodide not only inhibits currents at positive potentials but enhances N-type current at negative potentials. Enhancement was also observed in cell-attached patches. These findings provide evidence for N-type Ca^{2+}-current enhancement by a classical neurotransmitter. Moreover, enhancement and inhibition of current by oxotremorine methiodide mimics modulation observed with direct application of a low concentration of arachidonic acid (AA). Although no transmitter has been reported to use AA as a second messenger to modulate any Ca^{2+} current in either neuronal or nonneuronal cells, we nevertheless tested whether a fatty acid signaling cascade was involved. Blocking phospholipase C, phospholipase A$_2$, or AA but not AA metabolism minimized muscarinic modulation of N-type current, supporting the participation of these molecules in the slow pathway. A role for the G protein G$_q$ was also confirmed by blocking muscarinic modulation of Ca^{2+} currents with anti-G$_{q\alpha}$ antibody. Our finding that AA participates in the slow pathway strongly suggests that it may be the previously unknown diffusible second messenger.

bovine serum albumin | calcium channel | G$_q$ protein | M$_1$ muscarinic receptor | phospholipase A$_2$ |

We have used neonatal rat superior cervical ganglion (SCG) neurons to characterize a slow-acting signal transduction cascade that mediates N-type current modulation by neurotransmitters such as acetylcholine (1). The cell bodies of neonatal SCG neurons are enriched in both N-type Ca^{2+} channels and muscarinic receptors (2). In these cells, cholinergic agonists inhibit Ca^{2+} currents by two pathways (3). The first involves M$_2$/M$_4$ muscarinic receptors (4, 5) inhibiting N-type current via a membrane-delimited, voltage-dependent, fast (maximal within seconds) pathway (6–8). Membrane-delimited, voltage-independent inhibition is not present in the neonate (7). The slow pathway, previously called the sman pathway (8, 9), is voltage-independent and slower (taking many seconds), inhibiting both L- and N-type currents (10–11). M$_1$ muscarinic receptors (4, 5), the pertussis toxin (PTX)-insensitive G protein G$_q$ (4, 12, 13), and an unknown diffusible second messenger (11) mediate this slow pathway of current inhibition. Initial tests to determine whether inositol 1,4,5-trisphosphate, cAMP, cGMP, protein kinase C, cAMP-dependent protein kinase A, or metabolites of arachidonic acid (AA) participate in the pathway were negative, suggesting that they do not mediate the M$_1$ effect (6, 8, 10, 11, 14–16). Low levels of intracellular Ca^{2+} are

required, suggesting the involvement of a Ca^{2+}-dependent molecule, e.g., calmodulin, a phosphatase, and/or a phospholipase (10, 11).

Details of downstream molecular involvement in the slow pathway are unknown, and despite a decade of research the diffusible second messenger remains unidentified. In neurons and recombinant systems, M$_1$ muscarinic receptors couple to G$_q$-like G proteins to stimulate phospholipase activity, resulting in the liberation of AA (17–21). Although AA metabolites have been tested, AA itself has not been examined as a mediator of the slow pathway. Our recent characterization of the action of AA in SCG neurons showed that at negative test potentials AA enhances N-type current, whereas at positive potentials AA-induced inhibition dominates (22–24). Furthermore, metabolism of AA seems unnecessary for its inhibitory effects (24–26). Because the characteristics of AA-induced current inhibition are similar to those of oxotremorine methiodide (oxo-M), we examined whether AA might be the unidentified diffusible second messenger.

Materials and Methods

Preparation of acutely dissociated neonatal (1- to 3-day-old) Sprague–Dawley rat SCG neurons and current recording conditions have been described (3, 24). We have found previously that muscarinic inhibition of the peak current in neonatal SCG neurons by the slow pathway shows the same characteristics observed in the adult (3). To isolate the actions of the diffusible second-messenger pathway on N-type current, cells were preincubated for at least 5 h with 500 ng/ml PTX, which removes inhibition of N-type current by activated M$_2$/M$_4$ muscarinic receptors coupling to the PTX-sensitive, membrane-delimited pathway (4, 6, 7). Including the L-type Ca^{2+}-channel antagonist nimodipine (NMN, 1 μM) in the bath minimized the small amount of L-type current present in SCG neurons. Under these conditions, N-type current dominated the whole-cell current. In some experiments, cells were pretreated with 1 μM ω-conotoxin GVIA for at least 20 min to block N-type Ca^{2+}-channel activity. The membrane voltage was held at −90 mV and stepped to +10 mV for 20 ms unless otherwise indicated. Command pulses were delivered at 4-s intervals. Current amplitudes were measured 15 ms after the start of the test pulse. Data are expressed as the percent change in current ± SEM. Statistical significance was determined by either a two-way Student's t test for two means or a two-tailed paired t test with $P < 0.05$ considered significant. The analysis programs used were PATCH (Cambridge Electronic Design, Cambridge, U.K.), EXCEL (Microsoft), and ORIGIN (Microcal Software, Northampton, MA).

NEUROSCIENCE

The external solution consisted of 20 mM barium acetate, 125 mM N-methyl-D-glucamine-aspartate, 10 mM Hepes, and 0.0005 mM tetrodotoxin (293 mOsM). Barium acetate was used to minimize whole-cell Ba^{2+} current contamination with Cl^- currents. The pipette solution consisted of 123 mM Cs-aspartate, 10 mM Hepes, 0.1 mM 1,2-bis(O-aminophenoxy)ethane-N,N,N',N'-tetraacetic acid, 5 mM $MgCl_2$, 4 mM ATP (Sigma), and 0.4 mM GTP (Sigma) (264 mOsM). The pH of each solution was adjusted to 7.5 with CsOH.

As required for each experiment, drugs were introduced by bath application unless otherwise indicated. Phospholipase antagonists were used at concentrations shown to have just maximal or submaximal inhibition in either the SCG or other cell systems; supramaximal concentrations were avoided to minimize nonspecific effects. Arachidonic acid (AA, Nu Chek Prep, Elysian, MN), indomethacin 5,8,11-eicosatriynoic acid and U-73122 (Biomol, Plymouth Meeting, PA), oleyloxyethyl phosphocholine (OPC, Calbiochem), and NMN and 7,7-dimethyl-5,8-eicosadienoic acid (Sigma) were prepared from stock solutions made up in 100% ethanol and diluted with the bath solution to a final ethanol concentration <0.17%, a concentration with no significant effect on currents (24). Stocks of anti-$G_{q/11}$ (2.2 mg/ml, directed at the homologous region in the α-subunit C terminus) and anti-G_q (2.2 mg/ml, directed at amino acids 115–133 of the rabbit α-subunit) antibodies and nonimmunized IgG (6.53 mg/ml) were purchased from Calbiochem, diluted 1:1,000 with pipette solution, and dialyzed into the cell for 10 min after membrane breakthrough. Stocks of oxo-M, tetrodotoxin (Research Biochemicals, Natick, MA, or Sigma), and PTX (List Biological Laboratories, Campbell, CA) were made in double-distilled water and diluted at least 1,000 times with bath solution to their final concentration. For certain experiments, 1-amino-benzotriazole (Biomol) and BSA (essentially fatty acid-free, Sigma) were added directly to either the pipette or bath solution.

Results

If AA mediates M_1 receptor signaling, then a muscarinic agonist such as oxo-M should mimic the actions of AA. We previously found that AA-induced current enhancement results from AA binding to a site that is extracellular or within the outer leaflet of the membrane, whereas inhibition is mediated intracellularly (23, 24). If oxo-M indeed does stimulate the liberation of AA from the inner leaflet of the membrane, some AA should flip to the outer leaflet based on principles of diffusion (27). Thus, oxo-M should not only inhibit current at positive test potentials but also enhance N-type current at negative voltages. To test this hypothesis, we measured whole-cell currents using alternating test potentials of −10 and +10 mV under conditions that isolate the actions of the slow pathway on N-type current (see *Materials and Methods*).

As observed (10, 11), oxo-M reversibly inhibited currents elicited at +10 mV (Fig. 1 A–D); however, at −10 mV, a potential not examined previously, oxo-M enhanced current. Comparable to our findings with AA (23, 24), these changes were maintained over time (Fig. 1C). The reversibility of this enhancement could not be determined because of technical problems. We therefore used 110 mM Ba^{2+} as the charge carrier to determine whether oxo-M enhanced unitary currents at +10 mV, a voltage equivalent to −10 mV under whole-cell conditions (3, 24). After bath application of 100 μM oxo-M, currents in multichannel patches increased 2.2 ± 0.6-fold ($n = 3$). Contrasting results were found in two patches that received additional bath solution rather than oxo-M. The mean ensemble current amplitude decreased in one patch from 0.32 to 0.08 pA and did not change in the second (0.026 versus 0.025 pA), indicating that enhanced current was due to oxo-M stimulating the slow pathway rather than a nonspecific "flow" effect. Consistent with whole-cell data, we previously found that currents from multichannel
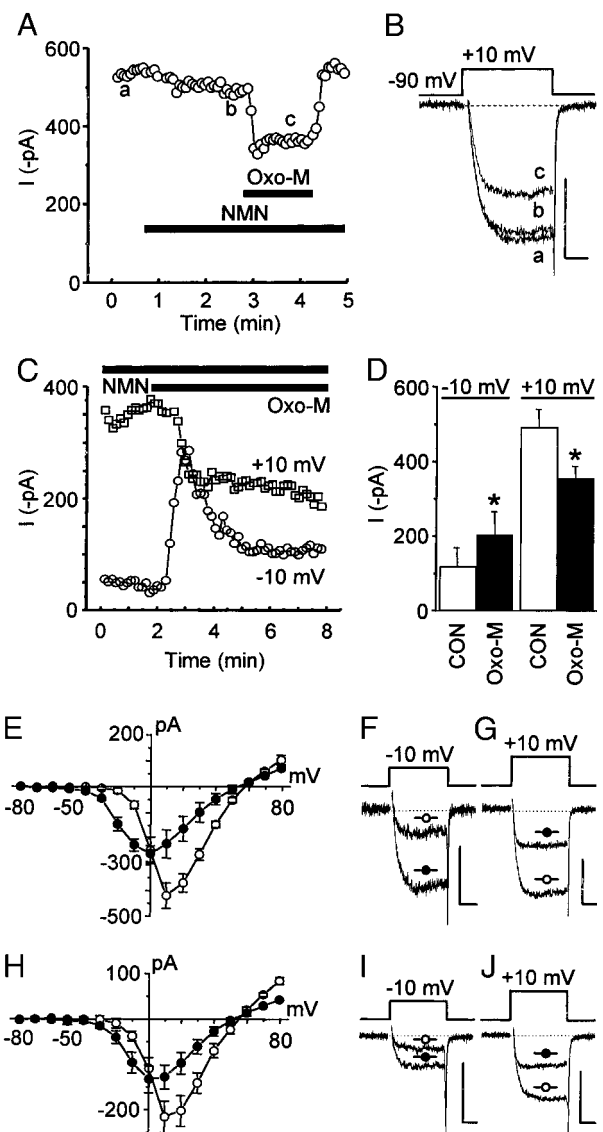
Fig. 1. The muscarinic agonist oxo-M and AA similarly enhance and inhibit whole-cell Ba^{2+} currents. In cells pretreated with PTX for at least 5 h, oxo-M (10 μM) reversibly inhibits N-type currents in the continued presence of 1 μM NMN. This inhibition is seen in the plot of current versus time (*A*) and in individual sweeps (*B*) taken where noted (a–c). (*C*) To test whether oxo-M (3 μM) enhances N-type current at negative voltages and inhibits at positive voltages, alternating 20-ms test potentials to −10 (to monitor enhancement) and +10 mV (to monitor inhibition) were applied every 4 s. After oxo-M, the initial current increase relaxes at −10 mV, most likely because of some concurrent inhibition at this voltage. Over time, a net sustained enhancement at −10 mV and inhibition at +10 mV is observed. (*D*) Summary of oxo-M-induced current modulation ($n = 6$). *, $P < 0.05$, compared with paired control (CON). (*E*) Summary of current–voltage relationships in the absence (○, $n = 4$) and presence (●, $n = 4$) of 3 μM oxo-M. Selected traces illustrate the oxo-M-induced changes in currents at −10 (*F*) and +10 mV (*G*). (*H*) Summary of current–voltage relationship in the absence (○, $n = 4$) and presence (●, $n = 4$) of 5 μM AA. Selected traces illustrate the AA-induced changes in currents at −10 (*I*) and +10 mV (*J*). (Scale bars for *B, F, G, I* and *J*, 250 pA, 5 ms.)

patches at a test potential of +30 mV, equivalent to +10 mV in whole-cell recordings, significantly decreased by ≈55% (3). Moreover, when whole-cell current–voltage plots were compared, the unique pattern of current enhancement at negative
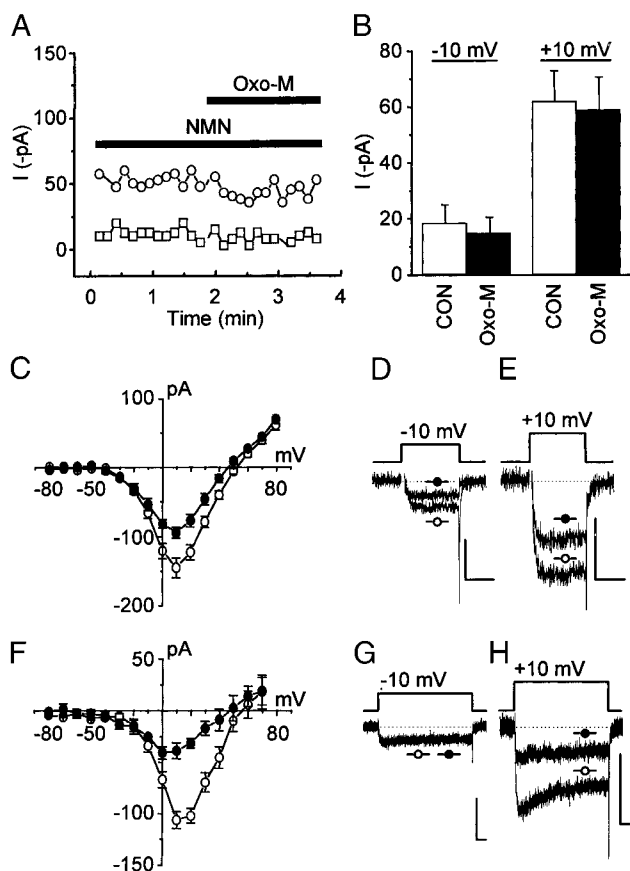
Fig. 2. ω-Conotoxin GVIA abolishes oxo-M- and AA-induced enhancement of N-type current. To test whether N-type current carries enhancement, PTX-treated cells were preincubated for at least 30 min in Tyrode's solution (37°C) containing ω-conotoxin GVIA (1 μM), which irreversibly blocks N-type Ca^{2+}-channel activity (12). (*A*) Recordings at −10 (□) and +10 mV (○) in the presence of NMN (1 μM) showed little current, and applying 3 μM oxo-M did not change current amplitude significantly over time. (*B*) Summary data from time-course experiments (*n* = 5). CON, control. (*C*) Enhancement of current by 3 μM oxo-M (●) observed in current–voltage plots is lost compared with control (○), whereas inhibition of the ω-conotoxin GVIA-resistant current remains. In this series of experiments, L-type current was left uninhibited (no NMN in the bath) and used as a positive control, because oxo-M also inhibits L-type Ca^{2+}-channel activity (24, 30). Selected traces illustrate the oxo-M-induced changes in currents at −10 (*D*) and +10 mV (*E*). (*F*) Under similar conditions, the actions of 10 μM AA (●) compared with control (○) mimicked those of 3 μM oxo-M. Test pulse length, 100 ms. Selected traces illustrate the AA-induced changes in currents at −10 (*G*) and +10 mV (*H*). (*C* and *F*) *n* = 3–8 cells per data point. (Scale bars for *D*, *E*, *G*, and *H*: 100 pA, 10 ms.)

voltages and inhibition at positive voltages was remarkably similar for oxo-M (Fig. 1 *E–G*) and AA (Fig. 1 *H–J*).

In the above whole-cell experiments, L-type current was minimized, indicating that at −10 mV oxo-M induces an increase in N-type current. It is possible, however, that oxo-M stimulates the activity of additional Ca^{2+}-channel phenotypes such as mid- to low-threshold channels (28, 29). These channels normally inactivate faster than N-type channels, yet the currents enhanced by oxo-M do not inactivate rapidly (Fig. 1*F*). This finding argues against the enhanced current originating from mid- or low-threshold Ca^{2+} channels. Nevertheless, to test whether N-type current is enhanced, cells were preincubated with ω-conotoxin GVIA to block N-type channel activity (7). After this pretreatment, oxo-M-induced current enhancement at −10 mV and inhibition at +10 mV were lost (Fig. 2 *A* and *B*). Furthermore, oxo-M-induced enhancement, observed at negative potentials in

current–voltage plots (Fig. 2 *C* and *D*), was minimized under conditions where AA-induced enhancement is lost (Fig. 2 *F* and *G*). Taken together, these results demonstrate that as with AA, oxo-M enhances N-type current at negative voltages, whereas at positive voltages inhibition prevails. Thus, by monitoring both current enhancement and inhibition, we took advantage of this unique current–voltage profile to examine further whether AA participates in the slow pathway.

Because AA and oxo-M had comparable effects on N-type current, we tested whether AA itself participates in N-type current modulation by oxo-M. To limit the availability of free AA during muscarinic receptor activation, we used an established strategy to sequester free fatty acids. BSA rapidly binds free AA (31). Although BSA in the bath cannot cross the cell membrane, it acts as a sink for AA at the outer membrane–extracellular fluid interface. After its liberation from phospholipids, AA should diffuse from the inner to the outer lipid layer of the cell membrane (27). Once there, BSA binds AA, creating a concentration gradient that results in net movement of AA from the cell. BSA in the bath thus should limit the availability of any AA released from cell membranes after muscarinic stimulation. With BSA in the bath (Fig. 3 *A–C*), oxo-M-induced current enhancement at −10 mV and inhibition at +10 mV were no longer significant (*P* > 0.05 using a two-tailed paired *t* test; *n* = 4–5 pairs per group). In addition, dialyzing BSA into the cell significantly reduced current inhibition by oxo-M (20.8 ± 4.7% with BSA versus 35.2 ± 2.9% for control). These results support the hypothesis that oxo-M stimulates the liberation of AA from phospholipids. However, further metabolism of AA appears unnecessary, because oxo-M (10 μM) inhibited currents by 25 ± 2.4% (*n* = 7) in cells simultaneously pretreated with indomethacin (10 μM), 5,8,11-eicosatriynoic acid (5 μM), and the suicide substrate 1-aminobanzotriazole (3 mM) (24), antagonists of the cyclooxygenase, lipoxygenase, and the cytochrome P450 oxygenase pathways, respectively. This inhibition did not (*P* > 0.05) differ significantly from that of matched controls (28 ± 3.6%, *n* = 5).

Because phospholipase A$_2$ (PLA$_2$) directly cleaves AA from phospholipids and stimulation of M$_1$ receptors is reported to activate PLA$_2$ (17, 19), we examined whether inhibiting PLA$_2$ activity with OPC minimizes the actions of oxo-M. In the sample time course and representative traces shown in Fig. 3 *D* and *E*, respectively, current inhibition by oxo-M is lost once OPC (10 μM) is introduced into the bath. In a second series of experiments, oxo-M-induced current enhancement and inhibition, observed in current–voltage plots, were no longer significant in the continued presence of OPC (Fig. 3 *D–F*). In contrast, OPC had no effect on inhibition of currents measured at +10 mV when AA (5 μM) rather than oxo-M was applied directly to the bath; AA decreased currents by 70.5 ± 8.1% (*n* = 4). Moreover, OPC had no apparent effect on oxo-M-induced inhibition of N-type current by the membrane-delimited pathway in time-course studies when it was left active (no PTX pretreatment). However, current inhibition by the slow pathway was lost (data not shown). These results suggest that OPC does not disrupt the activity of membrane-associated proteins such as muscarinic receptors or G proteins. Furthermore, under these latter conditions, substitution of OPC with 100 μM 7,7-dimethyl-5,8-eicosadienoic acid, another PLA$_2$ inhibitor, also significantly reduced (*P* < 0.05, using a two-tailed *t* test for two means; *n* = 4–9 recordings per group) the inhibitory actions of oxo-M (control inhibition, 42 ± 3%; in the presence of 7,7-dimethyl-5,8-eicosadienoic acid, 18 ± 4%).

Last, we used a prepulse protocol (8, 32, 33) to compare the effects of OPC on voltage-dependent versus voltage-independent muscarinic inhibition (Fig. 4). Because current inhibition by the slow pathway is independent of voltage, OPC should antagonize this component of oxo-M induced inhibition
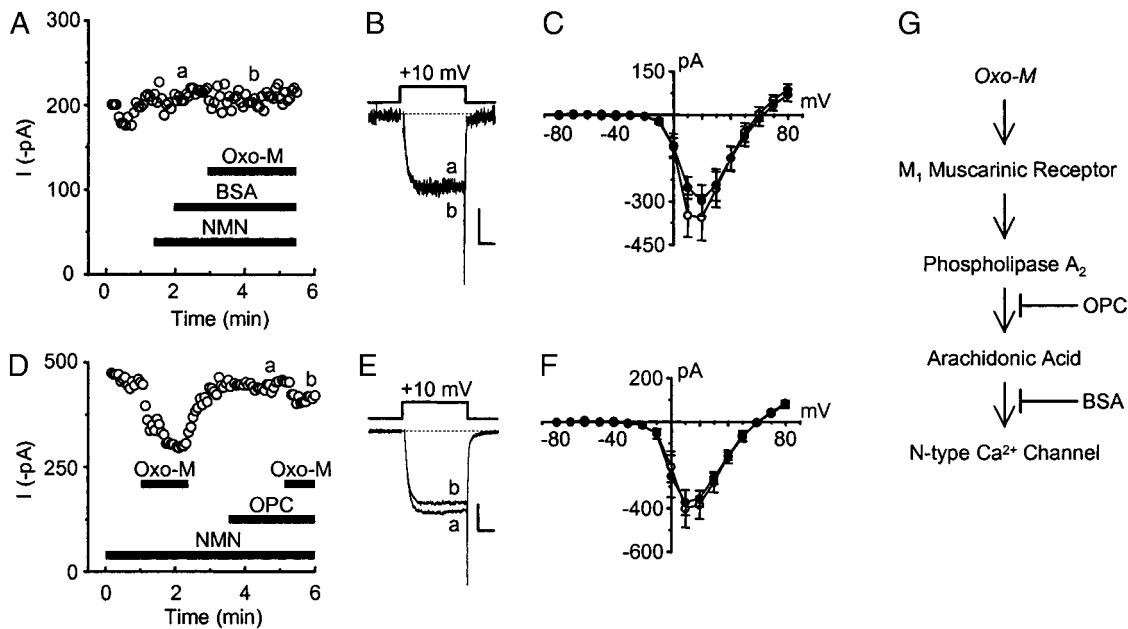
Fig. 3. Antagonizing the activity of AA or PLA$_2$ prevents modulation of N-type current by oxo-M. BSA (1 mg/ml) in the bath minimized current modulation by 10 μM oxo-M. This loss of effect can be observed in the plot of current (measured at +10 mV) versus time (*A*) and in selected sweeps (*B*) taken from *A*, where indicated. A similar loss of effect by oxo-M (3 μM) occurs in current–voltage plots (*C*, *n* = 4–5 recordings per data point). (*C*) NMN + BSA, ○; NMN, BSA + oxo-M, ●. (*D*) The activity of PLA$_2$ was inhibited with the selective antagonist OPC (10 μM). This sample time course shows initial current inhibition by 10 μM oxo-M, measured at +10 mV. OPC by itself in the bath did not affect whole-cell currents. In the continued presence of OPC and NMN, oxo-M no longer inhibited whole-cell currents. These effects also can be seen in the selected traces (*E*) taken from *D* where indicated. (*F*) The presence of OPC also minimized 3 μM oxo-M-induced changes in the current–voltage relationship (*n* = 4 recordings per data point). (*F*) NMN + OPC, ○; NMN, OPC + oxo-M, ●. (Scale bars for *B* and *E*: 100 pA, 5 ms.) (*G*) Schematic of the putative pathway.

selectively in neurons not treated with PTX. Under control conditions (−PP), 10 μM oxo-M inhibited currents 56 ± 5% (Fig. 4: *A*, filled circles; *B*, left traces; *C*, filled bars). After a prepulse (+PP), current inhibition was reduced to 24 ± 5% (Fig. 4: *A*, open circles; *B*, right traces; *C*, open bars), indicating that both voltage-dependent and voltage-independent components of inhibition are stimulated with agonist. With OPC in the bath, the magnitude of −PP inhibition by oxo-M decreased; current was inhibited 24 ± 5% from control levels (Fig. 4: *D*, filled circles; *E*, left traces; *F*, filled bars). Furthermore, all the oxo-M-induced inhibition could now be relieved with a prepulse (Fig. 4: *D*, open circles; *E*, right traces; *F*, open bars); no voltage-independent inhibition remained. These findings are consistent with OPC selectively antagonizing activation of the slow pathway without affecting voltage-dependent inhibition.

Thus we have shown that OPC antagonizes muscarinic modulation of current in four experiments: (*i*) studies of enhancement and inhibition observed in current–voltage plots; (*ii*) time-course studies examining inhibition in PTX-treated cells; (*iii*) time-course studies examining inhibition without PTX pretreatment (while inhibition by the membrane-delimited pathway remains); and (*iv*) prepulse-protocol experiments examining voltage-independent inhibition. Moreover, because OPC seems to have no effect up- or downstream from its putative site of action, directly on AA, or in any way that differs from other commonly used PLA$_2$ inhibitors, these experiments indicate that OPC is antagonizing PLA$_2$ activity selectively. Taken together, these results indicate that PLA$_2$ activity is required for muscarinic modulation of N-type current and further implicate AA as a participant of the slow pathway (Fig. 3*G*).

We next determined whether G$_{q/11}$-like G proteins couple to muscarinic receptors to mediate the slow inhibition of N-type current (Fig. 5*A*). When antibodies to G$_{q/11\alpha}$ or specific to G$_{q\alpha}$ were included in the pipette solution, current inhibition by 10 μM

oxo-M was lost in PTX-treated cells (Fig. 5 *C–E*). In contrast, dialyzing cells with nonimmunized IgG left the effects of oxo-M intact (Fig. 5 *B* and *E*). These findings support previous reports (12, 13) that G$_q$-like G proteins mediate the slow pathway.

PLA$_2$ activation can occur after G$_q$ activation of phospholipase C (PLC) (19). Therefore, to test whether PLC is also involved in the slow pathway, U-73122 (2.5 μM), a selective inhibitor of PLC with no effect by itself on currents (data not shown), was applied to the bath. In its presence, oxo-M-induced current inhibition was only 11.0 ± 6.1% (*n* = 6) compared with 35.2 ± 2.9% (*n* = 7) observed with control conditions (Fig. 5*E*). Although PLC seems to contribute to this pathway, downstream activation of protein kinase C does not, because the protein kinase C activator phorbol 12-myristate 13-acetate (500 nM) slightly enhanced rather than inhibited currents measured at +10 mV (control, 297 ± 60 pA, versus phorbol 12-myristate 13-acetate, 324 ± 54 pA; *n* = 4) as previously observed (11, 15).
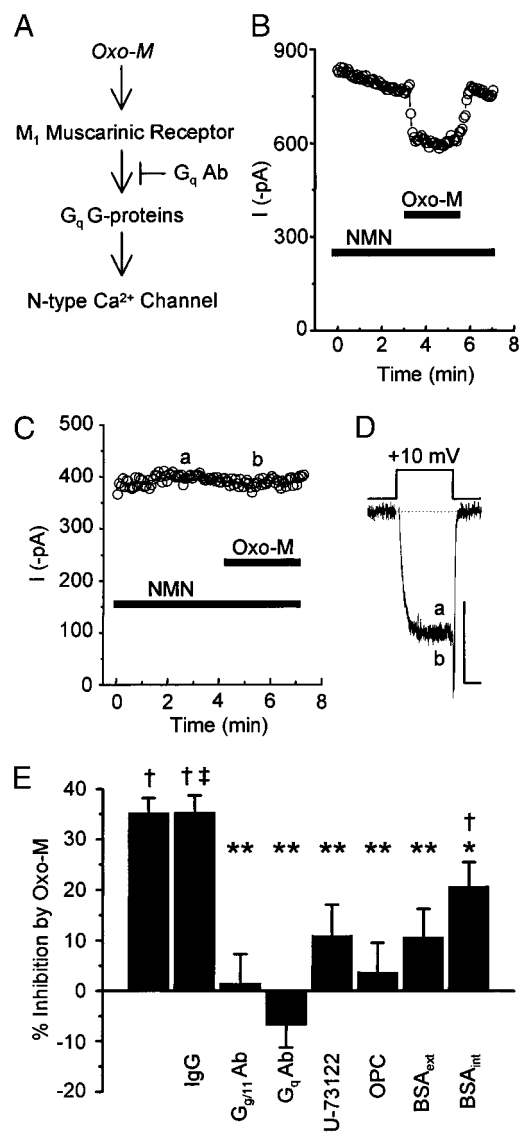
Discussion

In our examination of muscarinic inhibition of N-type Ca^{2+} current in SCG neurons by the slow pathway, we found that N-type current can also be enhanced by agonist; classical transmitters previously were known solely to inhibit this current (6, 10, 11). We have also characterized the mechanism for current modulation by identifying PLC, PLA$_2$, and AA as additional molecules involved in the slow pathway and by confirming a role for the G protein G$_q$ (12, 13). This conclusion is based on the finding that blocking any of these molecules minimizes muscarinic modulation of N-type current (Fig. 5). Moreover, oxo-M-induced current enhancement and inhibition (Fig. 1) mimic current modulation observed with direct application of AA.

Identifying AA as a participant in this pathway indicates that it may be the unidentified diffusible second messenger and may mediate both enhancement and inhibition of whole-cell N-type
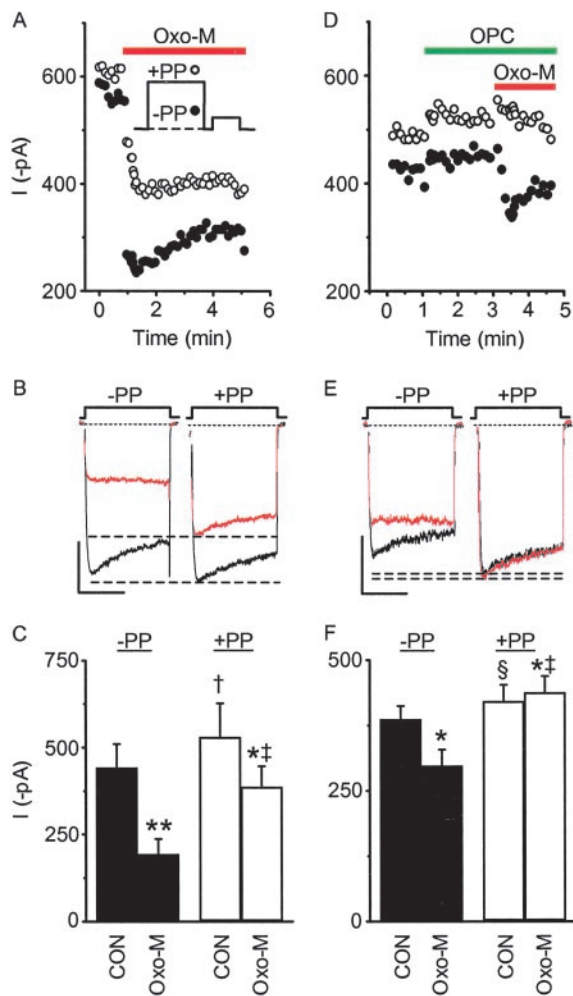
Fig. 4. OPC eliminates voltage-independent inhibition of whole-cell currents by oxo-M. (*A Inset*) Currents from −PTX-treated cells were generated by using a double-pulse protocol that alternated every 4 s between a 200-ms prepulse to +80 mV (+PP, ○) or no prepulse (−PP, ●). After a brief (5-ms) return to −90 mV, the cell was stepped to +10 mV for 100 ms. Current inhibition by 10 μM oxo-M had both voltage-dependent and voltage-independent components, as observed in the sample time course (*A*), corresponding selected sweeps (*B*), and summary histogram of mean current amplitude (*C*). (*B*) The magnitude of voltage-independent inhibition is shown in the right pair of traces as the difference between the dashed lines, which highlight the peak of control and oxo-M currents after a prepulse (+PP). (*C*) Oxo-M significantly decreased −PP (**, $P < 0.005$) and +PP (*, $P < 0.05$) currents compared with paired controls (CON), indicating the presence of voltage-dependent and independent inhibition. After a prepulse (+PP), significant facilitation of control (†, $P < 0.05$ compared with −PP by a one-tailed paired t test) and oxo-M currents (‡, $P < 0.01$) occurred. (*D–F*) When OPC (10 μM) was present in the bath, a small component of tonic inhibition remained as seen in a sample time course (*D*), individual sweeps (*E*), and the summary bar graph (§, $P < 0.05$, control/+PP versus control/−PP). Oxo-M (−PP) significantly decreased current in the presence of OPC (*, $P < 0.05$). Facilitation of current occurred in the presence of OPC and oxo-M (‡, $P < 0.01$), but voltage-independent inhibition by oxo-M was lost; all inhibition was relieved with a prepulse (*D*, ○; *E*, right traces; *F*, open bars; ‡, $P < 0.01$). Indeed a small but significant (*, $P < 0.05$) enhancement of current was observed (−4 ± 3% inhibition). (*B* and *E*) Control ± OPC, black; 10 μM oxo-M ± OPC, red. (Scale bars: vertical, 200 pA; horizontal, 50 ms.) (*C* and *F*) $n = 6$ recordings per group. Differences were analyzed by a two-tailed paired t test unless otherwise indicated.

Fig. 5. Antagonizing the activity of G_q-like G proteins, PLC, PLA_2, or AA inhibits the ability of oxo-M to modulate N-type current. (*A*) G_α antibodies were included in the pipette solution and dialyzed into the cell. (*B*) Dialyzing nonimmunized IgG did not significantly affect the ability of oxo-M to reversibly inhibit current, measured at +10 mV. Dialysis of antibodies to $G_{q\alpha}$ essentially blocked current inhibition as observed in the plot of current versus time (*C*) and in individual sweeps (*D*) taken where indicated from *C*. (Scale bars: 250 pA, 5 ms.) (*E*) Summary of changes in oxo-M-induced inhibition of whole-cell currents by various antagonists. Oxo-M reversibly inhibited whole-cell N-type currents 35.2 ± 2.9% ($n = 7$). Inhibition with IgG in the pipette was not significantly different from normal inhibition ($P > 0.05$). When antibodies to $G_{q/11\alpha}$ or $G_{q\alpha}$ were dialyzed into cells, current inhibition by oxo-M was minimized [1.5 ± 5.8% ($n = 5$) and −6.9 ± 4.4% ($n = 6$) inhibition, respectively]. Average oxo-M-induced inhibition with U-73122 (2.5 μM) in the bath was 11.0 ± 6.1% ($n = 6$); with OPC (10 μM), 6.6 ± 6.4% ($n = 5$); with BSA (1 mg/ml), 10.8 ± 5.5% ($n = 5$); and with BSA (1 mg/ml) in the pipette solution, 20.8 ± 4.7% ($n = 12$). †, $P < 0.05$, compared with paired, unstimulated currents; ‡, $P > 0.05$, compared with percent change by oxo-M with no additions; *, $P < 0.05$; **, $P < 0.001$, compared with percent change by oxo-M with no additions.

current. Moreover, this study and our previous ones (23, 24) indicate that under the conditions used AA itself rather than a metabolite modulates N-type current, suggesting a previously

uncharacterized signal transduction mechanism for altering neuronal excitability. This conclusion arises from studies demonstrating transmitter-induced enhancement of a variety of K^+ currents by a PLA_2–AA pathway that always involves AA metabolites (34–37). Modulation of Na^+ and Cl^- currents by AA after its liberation by transmitters has been implied but not

NEUROSCIENCE

demonstrated (38, 39). Our results, which complement biophysical (1) and biochemical (17, 19, 40) findings for M_1 receptor signaling, have not been observed previously; no transmitter has been reported to use AA to modulate any type of Ca^{2+} current in either neurons or nonneuronal cells. Whether AA acts directly on the channel or stimulates additional downstream molecules remains to be determined.

Because AA-induced enhancement occurs either extracellularly or in the outer membrane leaflet, whereas inhibition seems to occur at an intracellular site (23, 24), oxo-M-induced current enhancement and inhibition could be expressed independently of one another, adding complexity to N-type Ca^{2+}-channel modulation. Moreover, M_1 receptor-mediated N-type current modulation occurs at membrane potentials similar to those achieved during synaptic stimulation of the SCG, advancing the notion that liberation of AA from phospholipids may coordinate the modulation of electrical activity with underlying acute and long-term processes that are regulated by N-type Ca^{2+} current (41–43). Because free AA can diffuse across cell membranes and move into extracellular spaces, AA may participate in coordinating both pre- and postsynaptic events that underlie synaptic plasticity. For example, transmitter-induced AA release from membrane phospholipids has the potential to act retrogradely on target proteins located in presynaptic terminals. There, AA-induced current modulation would provide a previously uncharacterized mechanism for altering transmitter release, because Ca^{2+} influx through N-type channels stimulates release at many synapses (44).

Here we present evidence that AA may be the diffusible second messenger mediating N-type current modulation in SCG neurons; AA also may serve a similar role in the CNS. Within the CNS, cholinergic modulation of N-type current by an uncharacterized diffusible second-messenger pathway has been described in the prefrontal cortex, hippocampus, and striatum (2), where M_1 receptors are thought to play key roles in learning, memory, cognition, and Alzheimer's disease (45–47). Muscarinic stimulation of AA release has been reported for these same brain areas (19, 48, 49), suggesting that AA could be the messenger mediating modulation of Ca^{2+} currents. Other metabotropic receptors (50–52) that couple to G_q-like G proteins have been reported to modulate Ca^{2+} currents by an uncharacterized diffusible second-messenger pathway with properties similar to the slow pathway described in SCG neurons (50–53). Where examined, these receptors also stimulate AA release (54–56), suggesting that additional receptors may use AA to modulate Ca^{2+} currents. Our findings in the SCG together with those of previous CNS studies, implicate AA and the slow pathway as a major signaling mechanism used by G_q-coupled receptors to mediate transmitter-induced modulation of Ca^{2+}-channel activity and thus neuronal excitability.

1. Shapiro, M. S., Gomeza, J., Hamilton, S. E., Hille, B., Loose, M. D., Nathanson, N. M., Roche, J. P. & Wess, J. (2001) *Life Sci.* **68,** 2481–2487.
2. Levey, A. I. (1993) *Life Sci.* **52,** 441–448.
3. Liu, L. & Rittenhouse, A. R. (2003) *Br. J. Pharmacol.*, in press.
4. Bernheim, L., Mathie, A. & Hille, B. (1992) *Proc. Natl. Acad. Sci. USA* **89,** 9544–9548.
5. Shapiro, M. S., Loose, M. D., Hamilton, S. E., Nathanson, N. M., Gomeza, J., Wess, J. & Hille, B. (1999) *Proc. Natl. Acad. Sci. USA* **96,** 10899–10904.
6. Wanke, E., Ferroni, A., Malgaroli, A., Ambrosini, A., Pozzan, T. & Meldolesi, J. (1987) *Proc. Natl. Acad. Sci. USA* **84,** 4313–4317.
7. Plummer, M. R., Rittenhouse, A. R., Kanevsky, M. & Hess, P. (1991) *J. Neurosci.* **11,** 2339–2348.
8. Beech, D. J., Bernheim, L. & Hille, B. (1992) *Neuron* **8,** 97–106.
9. Zhou, J., Shapiro, M. S. & Hille, B. (1997) *J. Neurophysiol.* **77,** 2040–2048.
10. Beech, D. J., Bernheim, L., Mathie, A. & Hille, B. (1991) *Proc. Natl. Acad. Sci. USA* **88,** 652–656.
11. Bernheim, L., Beech, D. J. & Hille, B. (1991) *Neuron* **6,** 859–867.
12. Delmas, P., Abogadie, Fe, C., Dayrell, M., Haley, J., Milligan, G., Caulfield, M. P., Brown, D. A. & Buckley, N. J. (1998) *Eur. J. Neurosci.* **10,** 1654–1666.
13. Haley, J. E., Delmas, P., Offermanns, S., Abogadie, F. C., Simon, M. I., Buckley, N. J. & Brown, D. A. (2000) *J. Neurosci.* **20,** 3973–3979.
14. Bley, K. R. & Tsien, R. W. (1990) *Neuron* **2,** 379–391.
15. Shapiro, M. K., Zhou, J. & Hille, B. (1996) *J. Neurophysiol.* **76,** 311–320.
16. Hille, B. (1994) *Trends Neurosci.* **17,** 531–536.
17. Conklin, B. R., Brann, M. R., Buckley, N. J., Ma, A. L. & Bonner, T. I. (1988) *Proc. Natl. Acad. Sci. USA* **85,** 8698–8702.
18. Bernstein, G., Blank, J. L., Smrcka, A. V., Higashijima, T., Sternweis, P. C., Exton, J. H. & Ross, E. M. (1992) *J. Biol. Chem.* **267,** 8081–8088.
19. Tence, M., Cordier, J., Premont, J. & Glowinski, J. (1994) *J. Pharmacol. Exp. Ther.* **269,** 646–653.
20. Biddlecome, G. H., Berstein, G. & Ross, E. M. (1996) *J. Biol. Chem.* **271,** 7999–8007.
21. Bymaster, F. P., Calligaro, D. O. & Falcone, J. F. (1999) *Cell. Signalling* **11,** 405–413.
22. Liu, L. & Rittenhouse, A. R. (2000) *J. Physiol. (London)* **525,** 391–404.
23. Barrett, C. F., Liu, L. & Rittenhouse, A. R. (2001) *Am. J. Physiol.* **280,** C1306–C1381.
24. Liu, L., Barrett, C. F. & Rittenhouse, A. R. (2001) *Am. J. Physiol.* **280,** C1293–C1305.
25. Hatton, C. J. & Peers, C. (1998) *Brain Res.* **787,** 315–320.
26. Keyser, D. O. & Alger, B. E. (1990) *Neuron* **5,** 545–553.
27. Kamp, F. & Hamilton, J. A. (1993) *Biochemistry* **32,** 11074–11086.
28. Meza, U., Bannister, R., Melliti, K. & Adams, B. (1999) *J. Neurosci.* **19,** 6806–6817.
29. Pemberton, K. E., Hill-Eubanks, L. J. & Jones, S. V. (2000) *Pflügers Arch. Eur. J. Physiol.* **440,** 452–461.
30. Mathie, A., Bernheim, L. & Hille, B. (1992) *Neuron* **8,** 907–914.
31. Spector, A. A. (1975) *J. Lipid Res.* **16,** 165–179.
32. Elmslie, K. S., Zhou, W. & Jones, S. W. (1990) *Neuron* **5,** 75–80.
33. Barrett, C. F. & Rittenhouse, A. R. (2000) *J. Gen. Physiol.* **115,** 277–286.
34. Piomelli, D., Volterra, A., Dale, N., Siegelbaum, S. A., Kandel, E. R., Schwartz, J. H. & Belardetti, F. (1987) *Nature* **328,** 38–43.
35. Schweitzer, P., Madamba, S. & Siggins, G. R. (1990) *Nature* **346,** 464–467.
36. Duerson, K., White, R. E., Jiang, F., Schonbrunn, A. & Armstrong, D. L. (1996) *Neuropharmacology* **35,** 949–961.
37. Vaughan, C. W., Ingram, S. L. & Connor, M. A. & Christie, M. J. (1997) *Nature* **390,** 611–614.
38. Fraser, D. D., Hoehn, K., Weiss, S. & MacVicar, B. A. (1993) *Neuron* **11,** 633–644.
39. Diener, M. & Gartmann, V. (1994) *Am. J. Physiol.* **266,** G1043–G1052.
40. Del Rio, E., Bevilacqua, J. A., Marsh, S. J., Halley, P. & Caulfield, M. P. (1999) *J. Physiol. (London)* **520,** 101–111.
41. Marrion, N. V. & Tavelin, S. J. (1998) *Nature* **395,** 900–905.
42. Brosenitsch, T. A. & Katz, D. M. (2001) *J. Neurosci.* **21,** 2571–2579.
43. Rittenhouse, A. R. & Zigmond, R. E. (1999) *J. Neurobiol.* **40,** 137–148.
44. Dunlap, K., Luebke, J. I. & Turner, T. J. (1995) *Trends Neurosci.* **18,** 89–98.
45. Durieux, M. E. (1996) *Anesthesiology* **84,** 173–189.
46. Stewart, A. E., Yan, Z., Surmeier, D. J. & Foehring R. C. (1999) *J. Neurophysiol.* **81,** 72–84.
47. Growdon, J. H. (1997) *Life Sci.* **60,** 993–998.
48. Reichman, M., Nen, W. & Hokin, L. E. (1987) *J. Neurochem.* **49,** 1216–1221.
49. Kanterman, R. Y., Ma, A. L., Briley, E. M., Axelrod, J. & Felder, C. C. (1990) *Neurosci. Lett.* **118,** 235–237.
50. Shapiro, M. S., Wollmuth, L. P. & Hille, B. (1994) *Neuron* **12,** 1319–1329.
51. Cardenas, C. G., Del Mar, L. P. & Scroggs, R. S. (1997) *J. Neurophysiol.* **77,** 3284–3296.
52. Kammermeier, P. J. & Ikeda, S. R. (1999) *Neuron* **22,** 819–829.
53. McCool, B. A., Pin, J.-P., Harpold, M. M., Brust, P. F., Stauderman, K. A. & Lovinger, D. M. (1998) *J. Neurophysiol.* **79,** 379–391.
54. Felder, C. C., Kanterman, R. Y., Ma, A. L. & Axelrod, J. (1990) *Proc. Natl. Acad. Sci. USA* **87,** 2187–2191.
55. Aramori, I. & Nakanishi, S. (1992) *Neuron* **8,** 757–765.
56. Zhu, M., Gelband, C. H., Moore, J. M., Posner, P. & Sumners, C. (1998) *J. Neurosci.* **18,** 679–686.